Porphyrins

International Edition: DOI: 10.1002/anie.201508033
German Edition: DOI: 10.1002/ange.201508033

A Rhodium-Mediated Contraction of Benzene to Cyclopentadiene: Transformations of Rhodium(III) *m*-Benziporphyrin

*Karolina Hurej, Miłosz Pawlicki, Ludmiła Szterenberg, and Lechosław Latos-Grażyński**

Abstract: *The contraction of benzene is one of an exclusive group of reactions where the cleavage of aromatic structure is of fundamental importance. Rhodium(III) m-benziporphyrin undergoes an unprecedented transformation of the built-in m-phenylene in which a perimeter carbon atom is extruded to form rhodium(III) 21-carbaporphyrin, stabilizing the formyl-unit-substituted rhodacyclopropane motif.*

The conversion of benzene or its derivatives into a cyclopentadiene ring has been rarely reported. Representative examples in which such challenge has been chemically addressed include: the photooxidation of benzene to form cyclopentadienecarboxyaldehyde,[1,2] a cleavage of aromatic rings with formation of metallacyclopentadiene complexes according to a retro-alkyne cyclotrimerization mechanism,[3] a reductive silylation of silyl-substituted arenes,[4] or insertion of tungsten into unstrained aromatic ring.[5] A notable room-temperature C–C bond fission of an arene by a metallacarborane has also been reported.[6] The C–C bond cleavage and rearrangement of benzene to a methylcyclopentenyl and a 2-methylpentenyl species by cleavage of the aromatic carbon skeleton through cooperation of multiple titanium centers has been also described.[7]

Porphyrinoids, including carbaporphyrinoids, provide a unique macrocyclic platform which is suitable to explore organometallic chemistry confined to a peculiar macrocyclic environment.[8–11] We have shown that palladium(II), gold(III), or rhodium(III) altered the fundamental framework of *p*-benziporphyrin **1**, allowing the facile intramolecular contraction of *p*-phenylene to cyclopentadiene yielding palladium(II), gold(III), or rhodium(III) 5,10,15,20-tetraaryl-21-carbaporphyrin derivatives (Scheme 1).[12–14] Apart from the examples listed above, the coordination chemistry of 21-carbaporphyrin includes only palladium(II) C(21)-methylated β-substituted 21-carbaporphyrin which demonstrates tetrahedral hybridization of the C(21) donor carbon atom[15] and palladium 21-carba-23-thiaporphyrin which adopts a trigonal geometry of the C(21) carbon donor (for the atom numbering scheme for 21-carbaporphyrin, see the Supporting Information).[16]

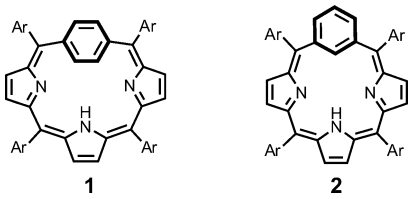

Scheme 1. 5,10,15,20-tetraarylbenziporphyrins **1** and **2**.

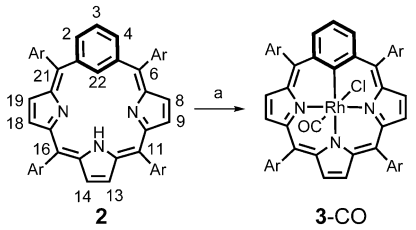

Scheme 2. Synthesis of **3**-CO (Ar = phenyl, *p*-tolyl, *p*-chlorophenyl). Reaction conditions: a) $[\{Rh(CO)_2Cl\}_2]$ (1 equiv), benzene, N_2, reflux, 2 h, 35% yield.

In this contribution we have probed the rhodium-triggered reactivity of a benzene ring embedded in *m*-benziporphyrin **2** (Scheme 2). Reaction of di-μ-chloro-tetracarbonyl-dirhodium(I) $[\{Rh(CO)_2Cl\}_2]$ with *m*-benziporphyrin **2** in benzene results in the formation of the six-coordinate Rh^{III} *m*-benziporphyrin **3**-CO (orange-brown; Scheme 2). The most notable feature of **3**-CO is the coordination of the rhodium(III) center through the unprotonated C(22) carbon atom of the benzene ring as inferred from the disappearance of the H(22) resonance signal in the ^{1}H NMR spectrum (Figure 1 A).

Rhodium(III) *m*-benziporphyrin **3**-CO was dissolved in dichloromethane and was subsequently placed on a silica gel slurry (with dichloromethane as the solvent) for column chromatography. After 12 h, it was found that compound **3**-CO had been converted into an aromatic compound **5** (Scheme 3), which was subsequently eluted with a dichloromethane/ethyl acetate solvent mixture. Compound **5** was eluted typically with some admixture of its degradation products, tentatively identified (by ^{1}H NMR spectroscopy; Figure 1 B) as rhodium(III) *m*-benziphlorins, which remains consistent with well-documented synthetic accessibility of *m*-benziphlorins.[17]

The progress of the transformation of **3**-CO into **5** was systematically followed by ^{1}H NMR spectroscopy. The yield of the conversion, evaluated by integration with respect to the internal standard, approaches circa 50%. Eventually we

[*] K. Hurej, Dr. M. Pawlicki, Dr. L. Szterenberg, Prof. Dr. L. Latos-Grażyński
Department of Chemistry, University of Wrocław
14 F. Joliot-Curie St., 50-383 Wrocław (Poland)
E-mail: lechoslaw.latos-grazynski@chem.uni.wroc.pl
Homepage: http://llg.chem.uni.wroc.pl

Supporting information for this article is available on the WWW under http://dx.doi.org/10.1002/anie.201508033.

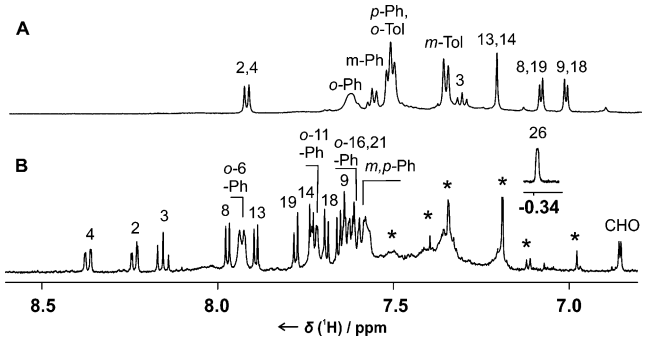

Figure 1. ^{1}H NMR spectra of A) **3**-CO (CD_2Cl_2, 290 K) and B) **5** ($CDCl_3$, 300 K). Resonance assignments follow the typical numbering of *m*-benziporphyrin (shown in Scheme 2 and Scheme 3). * Unidentified reaction products.

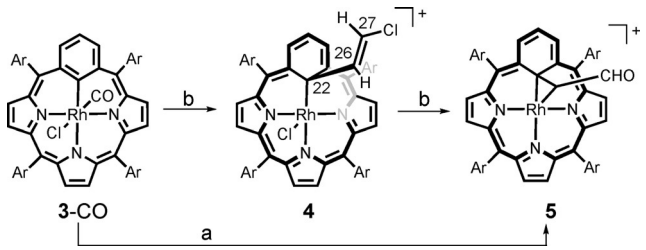

Scheme 3. The incorporation of a rhodacyclopropane motif into rhodium(III) *m*-benziporphyrin. Conditions: a) column chromatography (silica gel, dichloromethane, incubation time 12 h); b) reflux 12 h in dichloromethane.

realized that under typical conditions **5** exhibited limited stability, and consequently its identification could be achieved solely in solution by combining NMR spectroscopy (Figure 1 B) and HRMS. The synthetic scheme for the conversion of **3**-CO into rhodium(III) *m*-benziporphyrin **5**, which incorporates the rhodacyclopropane motif substituted with formyl, is demonstrated in Scheme 3. To account for determined properties of **5**, the DFT-optimized structure of the molecule was calculated (Figure 2).

The ^{1}H NMR spectrum of transient **5** reveals an increased multiplicity of carbaporphyrin resonance signals as compared to the C_s-symmetric **3**-CO substrate and reveals, according to the magnetic criteria,[18] the basic features of aromatic metallocarbaporphyrinoids (Figure 1 B).[9]

The DFT-optimized model of **5** (Figure 2) shows the structural constraints determined by NMR, including NOE connectivities. Such an architecture imposes a $Rh^{III}\cdots\eta^2$-C(22)C(26) arrangement, as reflected by the Rh–C(26) (2.031 Å) and Rh–C(22) (2.308 Å) bond lengths.[19,20] The C(22)–C(26) bond (1.479 Å) is longer than typical in ethene or η^2-ethene rhodium complexes.[19] The carbon atom C(22) displays a negligible degree of pyramidal distortion from a planar trigonal geometry, as reflected by the sum of respective bond angles [Σ = C(1)-C(22)-C(5) + C(1)-C(22)-C(26) + C(5)-C(22)-C(26)] which equals 357.9° (see Scheme 2 and Figure 2 for atom labelling). Calculations carried out for compound **5** predict a specifically distorted

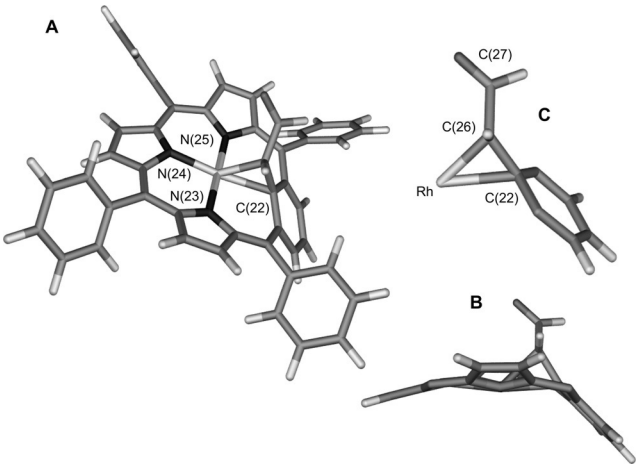

Figure 2. DFT-optimized molecular structure of **5** showing A) a perspective view, B) a side view with aryl groups omitted for clarity, and C) the geometry of the rhodacyclopropane in the fragment, which resembles a spiro[2.5]octa-4,6-diene.

environment of the coordinated internal carbon leading to a structure that is difficult to describe in terms of a simple valence-bond model.

In principle, the 21-carbaporphyrin moiety embedded in **3**-CO and **5** can be structurally related to two fundamental tautomers of *m*-benziporphyrin **2**, specifically **2**-1 and **2**-2, which can be differentiated by localization of the inner hydrogen atoms (Scheme 4).[21] A preference for local aromaticity within the *m*-phenylene is expected for **2**-1 and consequently the macrocyclic π-electron conjugation is disrupted. Tautomer **2**-2 is formally described by 18-π-electron conjugation pathway, and might therefore be expected to display aromatic features. The very large energy difference between **2**-1 and **2**-2 excludes the contribution of **2**-2 in tautomeric equilibria of *m*-benziporphyrin. Considering the diatropic properties of **5**, we could initially postulate that the structural framework of **2**-2 has been entrapped for the first time, presumably being stabilized by rhodium(III) coordination and the support of the bridging methylene unit. In support of this, the DFT-optimized model of **5** reveals that the C(22) center coordination geometry, although only modestly distorted from planarity, was still sufficiently distorted to limit

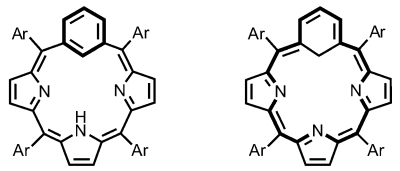

Scheme 4. Calculated energies (*E*; given in kcal mol^{-1}) and nucleus-independent chemical shifts (NICS; given in ppm) of two *m*-benziporphyrin isomers as obtained by DFT optimization.

the [6]annulene aromaticity and to prefer the macrocyclic 18 π-electron tautomer, as reflected by experimental and calculated chemical shifts. Thus, the aromaticity detected for **5** does not result from the energetic preference of the ligand, which would facilitate a hypothetical (**2**-1 to **2**-2) prearrangement step in coordination, but rather from the strong coordination of the rhodium(III) ion, as documented by the remarkable relocation of the C(22) resonance signal ($\delta_{C(22)}$ = 42.3 ppm) in **5** compared to its position in the C(22)–Rh fragment of **3**-CO ($\delta_{C(22)}$ = 143.3 ppm) and the C(22)–H component of **2** ($\delta_{C(22)}$ = 109.4 ppm), respectively.

The formation of **5** could not have been predicted considering the known properties of *m*-benziporphyrin complexes,[8–10,22] as we would have been puzzled by the source of the incorporated CHCHO fragment. Initially two hypotheses were considered. First, the CO ligand could have been transformed over the course of the redox processes, triggered by the provided reducing reagent, to eventually afford a fragment containing two carbon atoms.[23] Alternatively, efficient activation over the course of the reaction was considered, including the bond cleavage of esters, aldehydes, or ketones added or formed in solution. Reported carbon–carbon or carbon–hydrogen bond activation triggered by rhodium(III) or iridium(III) porphyrins provided grounds for this hypothesis.[24,25]

First, ^{13}CO-labelled rhodium complex **3**-^{13}CO was used as the substrate. The regular ^{1}H NMR and ^{13}C NMR spectroscopic patterns for the formation of compound **5** excluded the incorporation of a ^{13}C center (^{13}CO) into the CHCHO fragment. Under analogous conditions but in the presence of esters (ethyl acetate, ethyl ^{13}C(2)-acetate, [D_5]ethyl acetate, methyl acetate, ethyl propanoate), propanone, or ethanol, **3**-CO could not be converted into **5** or into a similar structure containing the rhodacyclopropane unit. Eventually, we established that **3**-CO converts into **5** during a refluxing process in dichloromethane through the initial formation of compound **4** (Scheme 3), in which a 2-chlorovinyl moiety has been trapped. A similar route of 2-chlorovinyl formation has been reported for cobalt(II) N-confused porphyrin.[26] The presence of the 2-chlorovinyl fragment has been undoubtedly proven by ^{1}H NMR experiments, in which resonance signals attributed to the unit attached at the C(22) position were detected (H(26) δ = 6.29 ppm, H(27) 5.59 ppm, $^3J_{trans}$ = 13.7 Hz;[27] C(26) δ = 134.5, C(27) 119.0 ppm, C(22) 81.5 ppm; Figure S45, see Scheme 3 for atom numbering). The crucial role of dichloromethane in the formation of the bridge was confirmed by replacing the regular solvent with its deuterated variant. No resonance signals for H(26) and H(27) were evident in the ^{1}H NMR spectrum of [D_2]-**4** and a comparison of the HRMS spectra (**4**: *m*/*z* calcd for $C_{50}H_{34}ClN_3Rh$ [**4**–HCl]$^+$ = 814.1496, found = 814.1495; [D_2]-**4**: *m*/*z* calcd for $C_{50}H_{33}D_2ClN_3Rh$ [[D_2]-**4** = 817.1700, found = 817.1692) verified the fundamental role of dichloromethane in the formation of the rhodacyclopropane unit. The subsequent prolonged reflux of **4** in dichloromethane (24 h) converted **4** into **5** confirming the crucial role of **4** as an intermediate in the formation of **5**.

Even deeper structural modifications were observed when **3**-CO was placed on a basic alumina, as this species immediately converts into a mixture of reddish-brown compounds (**6**, **7**-1, **7**-2; Scheme 5). The final separation of the compounds using column chromatography on silica gel (elution with dichloromethane) yielded two fractions, the first containing **6** (red-brown; 15 % with respect to **3**-CO) and the second the mixture of **7**-1 and **7**-2 (pink-brown; 10 % with respect to **3**-CO). Any further attempts to separate **7**-1 and **7**-2 using chromatography (including with HPLC) failed, as under chromatographic conditions these two species seem to be mutually convertible in the presence of silica gel or alumina. Significantly, the same aromatic species (**6**, **7**-1, **7**-2), were isolated once **5** instead of **3**-CO underwent transformation on the basic alumina column. In the context of these transformations, we can presume that the reaction of **3**-CO on alumina involves in fact two steps, including the intermediate compound **5** (Scheme 5).

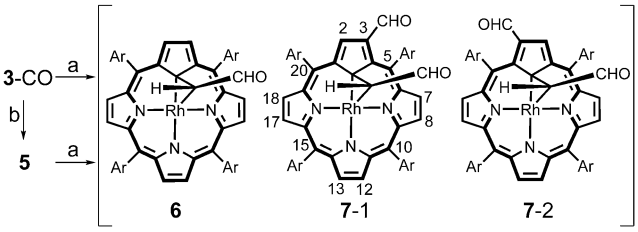

Scheme 5. Contraction of rhodium(III) *m*-benziporphyrin **3**-CO to rhodium(III) 21-carbaporphyrins **6**, **7**-1, and **7**-2. Conditions: a) column chromatography (alumina, dichloromethane as eluent); b) column chromatography (silica gel, dichloromethane as eluent, 12 h incubation time).

The ^{1}H NMR spectrum of **6** (Figure 3 A) resembles closely that of rhodium(III) μ-methylene 21-carbaporphyrin generated by contraction of rhodium(III) *p*-benziporphyrin **1**-Rh.[14] The ^{1}H NMR features of **7**–1 and **7**–2 (Figure 3 B) are instantly relatable to those of **6**. The presence of two

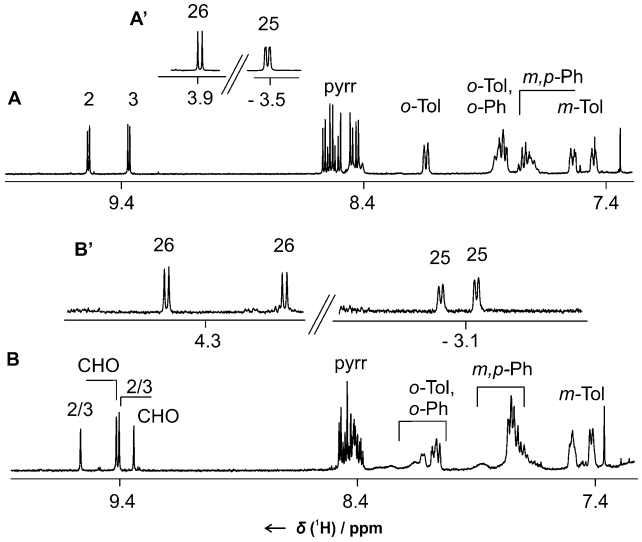

Figure 3. ^{1}H NMR spectra ($CDCl_3$, 300 K) of A) **6** and B) the mixture of **7**-1 and **7**-2. Insets (A′ and B′): the resonance signals for rhodacyclopropane protons. Assignments follow the typical numbering of 21-carbaporphyrin (numbering scheme for the CHCHO fragment shown in Figure 4 B).

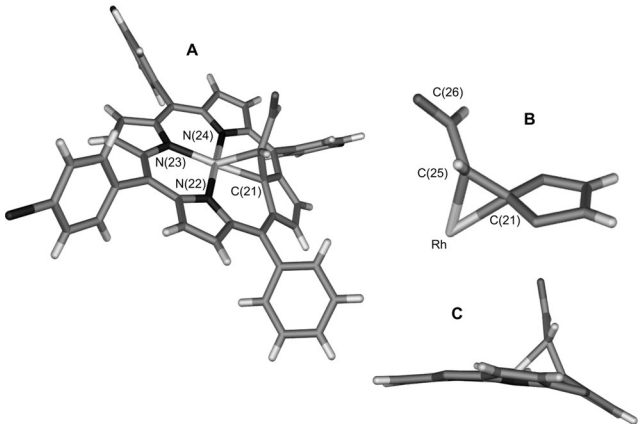

Figure 4. The X-ray crystal structure of **6**, showing A) a perspective view, B) the geometry of the rhodacyclopropane with partial atom labelling, and C) the side view (phenyl groups omitted for clarity). Selected bond lengths: Rh–N(22) 2.042(7) Å, Rh–N(23) 2.075(6) Å, Rh–N(24) 2.073(7) Å, Rh–C(21) 2.116(7) Å, Rh–C(25) 2.060(9) Å.

stereocenters in **7** (at the C(21) and C(25) positions; see Figure 4 for atom labelling) gives rise to two diastereomers **7**-1 and **7**-2, which can be readily differentiated from **6** by examination of their ^{1}H NMR spectra.

The X-ray crystal structure of **6** (Figure 4) bears some resemblance to metalloporphyrins modified by insertion of a single carbon atom into an M–N bond[28,29] and approaches closely the molecular structure of rhodium(III) μ-methylene 21-carbaporphyrin.[14] Such an architecture, which also incorporates some tetrahedral distortion around the C(21) carbon atom, imposes the $Rh^{III}\cdots\eta^2$-C(21)C(25) bonding mode.

The analysis of structural factors and the magnetic manifestations of macrocyclic aromaticity in the ^{1}H NMR spectrum of **6** is consistent with the presence of the rhodacyclopropane motif in **6** and **7**.

Mechanistic considerations suggest that compound **5** is activated toward nucleophilic addition. Once adsorbed on the basic alumina surface, **5** converts into nonaromatic **5**-OH acquiring the hydroxy group at the apical position (Scheme 6). The macrocycle of **5**-OH is actually a derivative of the porphyrinoid confined in **5** formally generated by addition of one molecules of water to **2**. The transformation of **5**-OH to **6** or **7** can be rationalized by a macrocyclic isomerization which results in conversion of 5-hydroxy cyclohexadiene into the bicyclic structure containing the fused cyclopropanol ring (Scheme 6). The subsequent rearrangement (via **5**-t_1) involves an extrusion of formaldehyde yielding **6** or elimination of H_2 (via **5**-t_2) to afford **7**.

The **5** to **6** (and **5** to **7**) transformation is accompanied by the relief of strain within the embedded 1,3-cyclohexadiene ring and finally by the formation of a new aromatic porphyrinoid systems.

In general terms, it is essential to recall that two isomeric carbaporphyrinoids *p*-benziporphyrin (**1**) and *m*-benziporphyrin (**2**) can be considered as the appropriate structural matrix to create 21-carbaporphyrin complexes. The isomers undergo conceptually related transformations (the inner core or perimeter extrusion of the carbon atom; Scheme 7), leading to a contraction of the phenylene rings to form cyclopentadiene moieties. For both isomers, ring contractions leads ultimately to the formation of the same molecular target—21-carbaporphyrin.

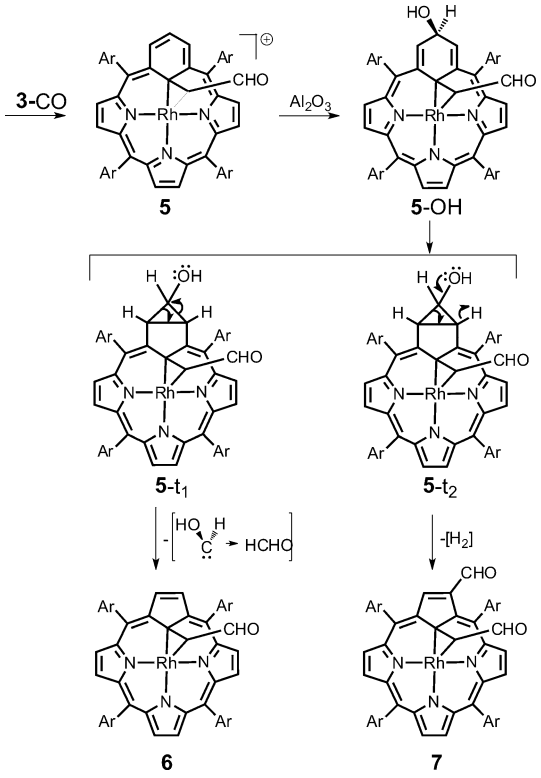

Scheme 6. Mechanistic insight into the contraction of rhodium(III) *m*-benziporphyrin **3**-CO to rhodium(III) 21-carbaporphyrin derivatives **6** and **7**.

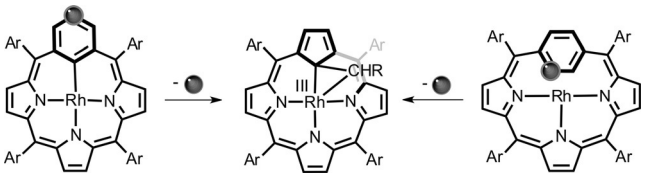

Scheme 7. Contraction of isomeric benziporphyrin complexes to form the common structural target of a rhodium(III) 21-carboporphyrin complex.

Acknowledgements

Financial support from National Science Centre (Grant 2012/04A/ST5/00593) is kindly acknowledged. DFT calculations were carried out at the Supercomputer Center of Poznań.

Keywords: aromaticity · carbaporphyrins · porphyrinoids · rhodium · ring contraction

How to cite: *Angew. Chem. Int. Ed.* **2016**, *55*, 1427–1431
Angew. Chem. **2016**, *128*, 1449–1453

[1] M. Luria, G. Stein, *Chem. Commun.* **1970**, 1650 – 1651.
[2] L. Kaplan, L. A. Wendling, K. E. Wilzbach, *J. Am. Chem. Soc.* **1971**, *93*, 3819 – 3820.
[3] R. M. Pope, S. L. VanOrden, B. T. Cooper, S. W. Buckner, *Organometallics* **1992**, *11*, 2001 – 2003.
[4] C. Krempner, H. Reinke, R. Wustrack, *Inorg. Chem. Commun.* **2007**, *10*, 239 – 242.
[5] A. Sattler, G. Parkin, *Nature* **2009**, *457-462*, 523 – 526.
[6] D. Ellis, D. McKay, S. A. Macgregor, G. M. Rosair, A. J. Welch, *Angew. Chem. Int. Ed.* **2010**, *49*, 4943 – 4945; *Angew. Chem.* **2010**, *122*, 5063 – 5065.
[7] S. Hu, T. Shima, Z. Hou, *Nature* **2014**, *512*, 413 – 415.
[8] B. Szyszko, L. Latos-Grażyński, *Chem. Soc. Rev.* **2015**, *44*, 3588 – 3616.
[9] M. Pawlicki, L. Latos-Grażyński in *Handbook of Porphyrin Science: with Applications to Chemistry, Physics, Materials Science Engineering, Biology and Medicine*, *Vol. 2* (Eds.: K. M. Kadish, K. M. Smith, R. Guilard), World Scientific Publishing, Singapore, **2010**, pp. 104 – 192.
[10] a) T. D. Lash, *Chem. Asian J.* **2014**, *9*, 682 – 705; b) T. D. Lash, *Org. Biomol. Chem.* **2015**, *13*, 7846 – 7878.
[11] M. Toganoh, H. Furuta in *Handbook of Porphyrin Science: with Applications to Chemistry, Physics, Materials Science Engineering, Biology and Medicine*, *Vol. 2* (Eds.: K. M. Kadish, K. M. Smith, R. Guilard), World Scientific Publishing, Singapore, **2010**, pp. 295 – 367.
[12] B. Szyszko, L. Latos-Grażyński, L. Szterenberg, *Angew. Chem. Int. Ed.* **2011**, *50*, 6587 – 6591; *Angew. Chem.* **2011**, *123*, 6717 – 6721.
[13] B. Szyszko, K. Kupietz, L. Szterenberg, L. Latos-Grażyński, *Chem. Eur. J.* **2014**, *20*, 1376 – 1382.
[14] A. Idec, L. Szterenberg, L. Latos-Grażyński, *Chem. Eur. J.* **2015**, *21*, 12481 – 12487.
[15] D. Li, T. D. Lash, *J. Org. Chem.* **2014**, *79*, 7112 – 7121.
[16] A. Berlicka, P. Dutka, L. Szterenberg, L. Latos-Grażyński, *Angew. Chem. Int. Ed.* **2014**, *53*, 4885 – 4889; *Angew. Chem.* **2014**, *126*, 4985 – 4989.
[17] M. Stępień, L. Latos-Grażyński, *Chem. Eur. J.* **2001**, *7*, 5113 – 5117.
[18] M. Pawlicki, L. Latos-Grażyński, *Chem. Asian J.* **2015**, *10*, 1438 – 1451.
[19] O. V. Zenkina, E. C. Keske, R. Wang, C. M. Crudden, *Organometallics* **2011**, *30*, 6423 – 6432.
[20] A. Vigalok, L. J. W. Shimon, D. Milstein, *Chem. Commun.* **1996**, 1673 – 1674.
[21] D. I. AbuSalim, T. D. Lash, *Org. Biomol. Chem.* **2014**, *12*, 8719 – 8736.
[22] M. Stępień, L. Latos-Grażyński, *Acc. Chem. Res.* **2005**, *38*, 88 – 98.
[23] X. X. Zhang, G. F. Parks, B. B. Wayland, *J. Am. Chem. Soc.* **1997**, *119*, 7938 – 7944.
[24] X. Song, K. S. Chan, *Organometallics* **2007**, *26*, 965 – 970.
[25] C. S. Chan, S. Y. Lee, K. S. Chan, *Organometallics* **2013**, *32*, 151 – 156.
[26] C. H. Hung, C. H. Peng, Y. L. Shen, S. L. Wang, C. H. Chuang, L. M. Lee, *Eur. J. Inorg. Chem.* **2008**, 1196 – 1199.
[27] F. Hruska, D. W. Mcbride, T. Schaefer, *Can. J. Chem.* **1967**, *45*, 1081 – 1087.
[28] Crystal data for **6** are given in the Supporting Information. CCDC 1420671 contain the supplementary crystallographic data for this paper. These data can be obtained free of charge from The Cambridge Crystallographic Data Centre.
[29] B. Chevrier, R. Weiss, J. C. Chottard, M. Lange, D. Mansuy, *J. Am. Chem. Soc.* **1981**, *103*, 2899 – 2901.

Received: August 27, 2015
Revised: September 24, 2015
Published online: December 8, 2015

